Chapter 4. Nonlinear Hyperbolic Problems

4.1. Introduction

Reading: Durran sections 3.5-3.6. Mesinger and Arakawa (1976) Chapter 3 sections 6-7.
Supplementary reading: Tannehill et al sections 4.4 and 4.5 – Inviscid and viscous Burgers equations.

Nonlinear problems creates two important problems in CFD:

1. They generate nonlinear instability.
2. New waves can be generated in nonlinear problems via nonlinear wave interaction.

The stability analysis we discussed in the previous Chapter refers to linear stability and linear instability – because they do not require nonlinearity in the equation.

The above two issues are specific to nonlinear equations.

Many processes in the atmosphere can be nonlinear – many physical processes, such as phase changes are nonlinear. In the Navier-Stokes equations, the most significant nonlinear term is the advection term.

The simplest equation including nonlinear advection is the Burges Equation:

Inviscid: $$\frac{\partial u}{\partial t} + u\frac{\partial u}{\partial x} = 0 \qquad \text{(Hyperbolic)} \qquad (1a)$$

Viscous: $\frac{\partial u}{\partial t} + u\frac{\partial u}{\partial x} = \upsilon\frac{\partial^2 u}{\partial x^2}$ (Parobolic) (1b)

We can rewrite the advection term $u\frac{\partial u}{\partial x} = \frac{\partial}{\partial x}\left(\frac{u^2}{2}\right)$ - the nonlinearity is often called quadratic nonlinearity.

There is a fundamental difference between the inviscid Burger's equation (1a) and the linear advection equation, $\frac{\partial u}{\partial t} + c\frac{\partial u}{\partial x} = 0$, we discussed in last chapter, where c is a constant.

1. In the linear problem, all points on the wave move at the same speed, c, the shape of the wave remain unchanged:

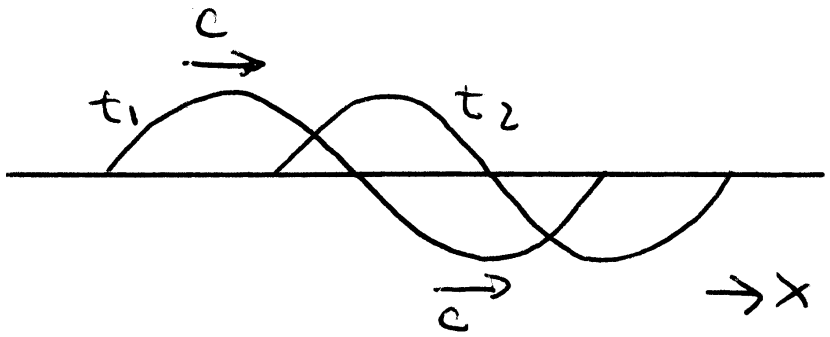

For a nonlinear equation (1b), the wave advects itself such the local speed depends on the wave amplitude and the shape of the wave change in time:

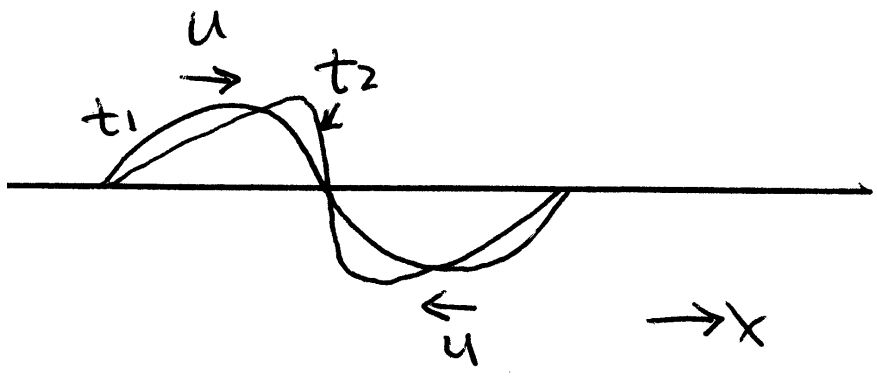

The process is called nonlinear steepening, and eventually results in shock waves and overturning if the flow is inviscid. In this case, the characteristics coalesce into a group where multiple values of u exist for a given x.

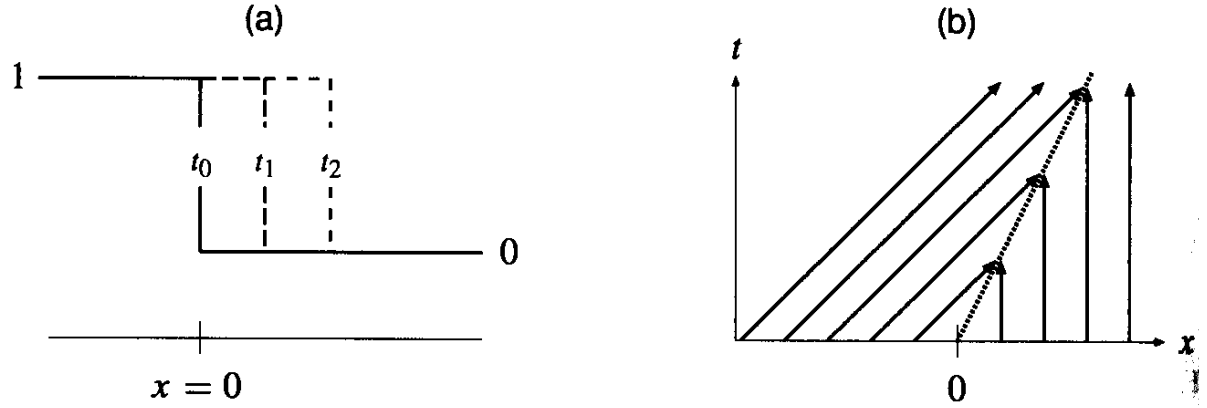

FIGURE 5.6. (a) An entropy-consistent shock, and (b) characteristic curves associated wit that shock. The trajectory of the jump is indicated by the heavy dashed line

2. Nonlinear problems create new waves modes. This was evident in the previous problem where we start with a single sine wave and ended up with a step-like function. Clearly the step function can be not represented by a

single wave → new waves have been generated! For nonlinear problems, the principle of superposition does not apply!

To illustrate this, consider $u = \sin(kx)$. Plug it into the advection term →

$$u\frac{\partial u}{\partial x} = k\sin(kx)\cos(kx) = k\sin(2kx)/2 .$$

Now the system contains a new wave – $\sin(2kx)$, whose wave number is $2k$, and wavelength is $L=\pi/k$, half of the wave length of the original $2\pi/k$.

The new wave can interact with itself and the original one, the process goes on and on and an entire spectrum of waves will result! This process is the source of aliasing error, to be discussed soon.

Despite of its nonlinear, Burger's equation has analytical solutions.

For the inviscid case, one of the examples is:

if $u(x, t=0) = -U\tanh(kx)$

then $u(x, t) = -U\tanh[\,k(x - ut)\,]$.

Note that the solution is an implicit function of u, and it has to be solved iteratively for the value of u.

For the viscous case, an example is:

if $u(x, t=0) = - U \tanh(kx)$

then the steady state solution is

$$u(x, t)= - U \tanh(ux/2\upsilon).$$

Here, dissipation of energy within the shock is exactly balanced by the conversion of kinetic energy from infinity.

References for exact solutions:

Platzman, 1964: Tellus, 4, 422-431.

Solution techniques

Many solution techniques discussed earlier for linear advection equation can be used for Burgers equation. We will not discuss them in details here, but we will look at the behaviors of the solutions:

Sample Solutions to the Inviscid Burgers' Equation

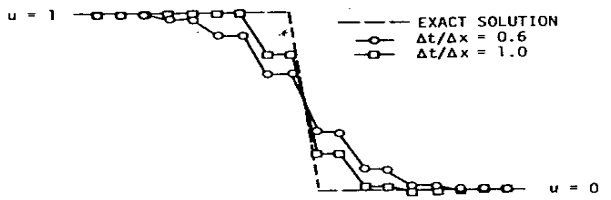

Figure 4-27 Numerical solution of Burgers' equation using Lax method.

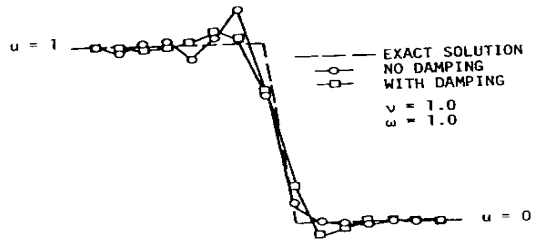

Figure 4-36 Solution for right-moving discontinuity time-centered implicit method, delta form.

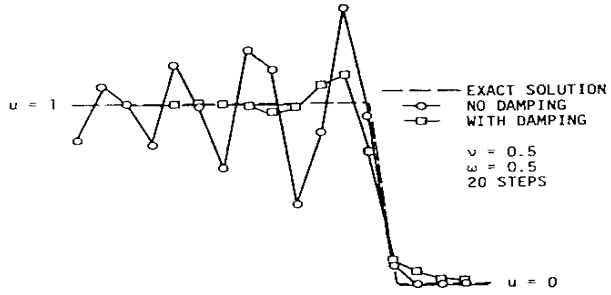

Figure 4-35 Solution of Burgers' equation using Beam-Warming (trapezoidal) method.

Because of the nonlinear steepening, the solution contains sharp gradient near the step – numerical schemes tend to perform poorly near sharp gradient, and most schemes, especially high order ones, generates small scale oscillations near the sharp gradient – monotonic schemes are particularly good at dealing with sharp gradient, because they are designed to prevent overshoot and undershoot from being generated.

With conventional schemes, there is a tendency for the small-scale noises to grow quickly and eventually destroy the solution or cause instability. Such instability occurs only in nonlinear problems, and was first discussed by the developer of NGM (Nested Grid Model, an early operational numerical weather prediction model of U.S.), Norman Phillips (1959), and the instability is called Nonlinear Instability.

4.2. Nonlinear Instability

Linear instability occurs when the linear stability criteria is violated, usually when Δt is too large.

Nonlinear instability occurs when waves shorter than $2\Delta x$ are generated and feed energy spuriously into the wavelengths near but larger than $2\Delta x$. The energy buildup becomes catastrophic.

The generation of waves with wavelength < $2\Delta x$ is a consequence of aliasing (c.f., p.35-42. Mesinger and Arakawa 1976. Read it!).

Aliasing:

Consider a function $u = \sin(kx)$.

We know that the shortest wave that can be represented by a grid has a wavelength of $2\Delta x$, corresponding to wavenumber $k = 2\pi/(2\Delta x) = \pi/\Delta x$ → the largest wavenumber is $k_{max} = \pi/\Delta x$ or $k_{max}\,\Delta x = \pi$.

We saw earlier for the nonlinear advection term $u\frac{\partial u}{\partial x}$

$$u\frac{\partial u}{\partial x} = k\sin(kx)\cos(kx) = k\sin(2kx)/2\,.$$

If $k = k_{max}$, then the new wave has a wave number of $2k_{max}$, corresponding to a wavelength of $(2\Delta x)/2 = \Delta x$ - too short to be represented on the grid!

Therefore, nonlinear interaction between waves can generate waves that are unresolvable by the original grid!

Then what happens to these unresolvable waves? They are spuriously presented, or aliased, as resolvable waves!

Consider a wave with W.L. = $4/3\Delta x$ ($<2\Delta x$). With only three grid points to represent one wavelength, it cannot tell it apart from the $4\Delta x$ wave. In fact, the grid misrepresents it as $4\Delta x$ wave!

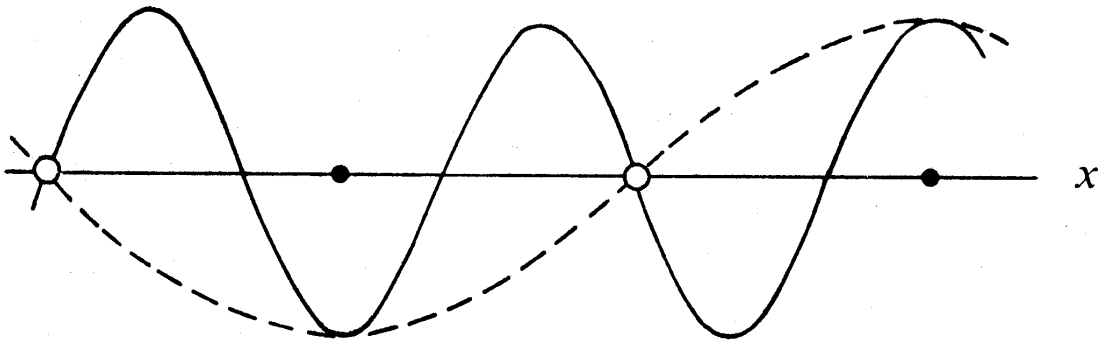

Figure 6.1 A wave of wave length $4\Delta x/3$, misrepresented by the finite difference grid as a wave of wave length $4\Delta x$.

Consider now a general case of a function u that contains harmonic components:

$$u = \sum_{u} u_n \rightarrow$$

nonlinear term will be of the form

$$\sin(k_1 x)\sin(k_2 x) = [\cos(k_1 - k_2)x - \cos(k_1 + k_2)x]/2$$

→ two new waves, $k_1 \pm k_2$, are created!

Even if the calculation is started with all wavelengths $\geq 2\Delta x$, waves $< 2\Delta x$ will be generated, through nonlinear interaction.

To generalize, let's write, knowing $k_{max}\,\Delta x = \pi$,

$$\cos(kx) = \cos[\, 2k_{max} - (2k_{max}-k)\,]\, x_i$$
$$= \cos\frac{2\pi x_i}{\Delta x}\cos(\frac{2\pi}{\Delta x} - k)x_i + \sin\frac{2\pi x_i}{\Delta x}\sin(\frac{2\pi}{\Delta x} - k)x_i .$$

Since $x_i = i\,\Delta x$, and i is integer, $\sin\frac{2\pi x_i}{\Delta x} = \sin\frac{2\pi i\Delta x}{\Delta x} = 0$, $\cos\frac{2\pi x_i}{\Delta x} = 1 \rightarrow$

$$\cos(kx_i) = \cos\{[2k_{\max} - k]x_i\}.$$

Knowing *only* those values at the grid points, we cannot distinguish between wavenumber k and $2k_{max}$-k, thus, if $k > k_{max}$ (W.L. $< 2\Delta x$), then k is really misrepresented as (or aliased as)

$$k^* = 2k_{\max} - k.$$

Thus, the aliased wave k^* is less than k_{max} by an amount equal to the amount by which k was greater then k_{max}:

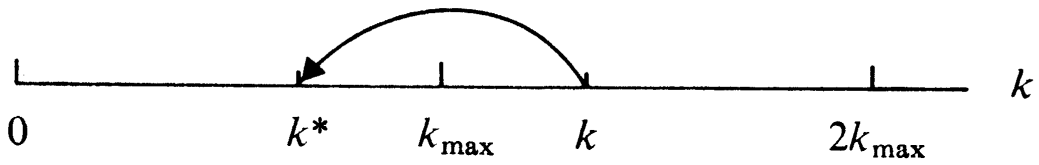

Figure 6.2 Misrepresentation of a wave number $k > k_{max}$, in accordance with (6.4).

Back to our example, let W.L. = 4/3 Δx, this is aliased as

$$k^* = 2\pi/(2\Delta x) - 2\pi/(4/3\Delta x) = 2\pi/(4\Delta x) \rightarrow 4\Delta x \text{ wave}$$

– the same as we saw earlier by the graphic means.

Note that the waves generated by aliasing are always near $2\Delta x$ – energy start to pile up in the form of short wave noises. In the next section, we will look at ways to control such pileup.

4.3. Controlling Nonlinear Instability

4.3.1. Consequences of N.L. Instability

If a flow contains many modes, it is useful to examine the distribution of energy (a measure of the amplitude of the modes) as a function of wavenumber:

$$E = \frac{\sum u'^{2}_{k}}{2}.$$

In a numerical simulation, aliasing occurs near $2\Delta x$ → energy is shifted to small scales and the short waves grow with time → nonlinear instability.

4.3.2. Filter Method

Phillips (1959) showed that catastrophic growth of wave disturbances can be prevented in a 2-level geostrophic model, by periodically applying a spectral filter, which eliminates waves shorter than or equal to $4\Delta x$.

The method decomposes the solution into Fourier modes (waves / harmonics), and recomposes them without hence eliminating the shortest waves.

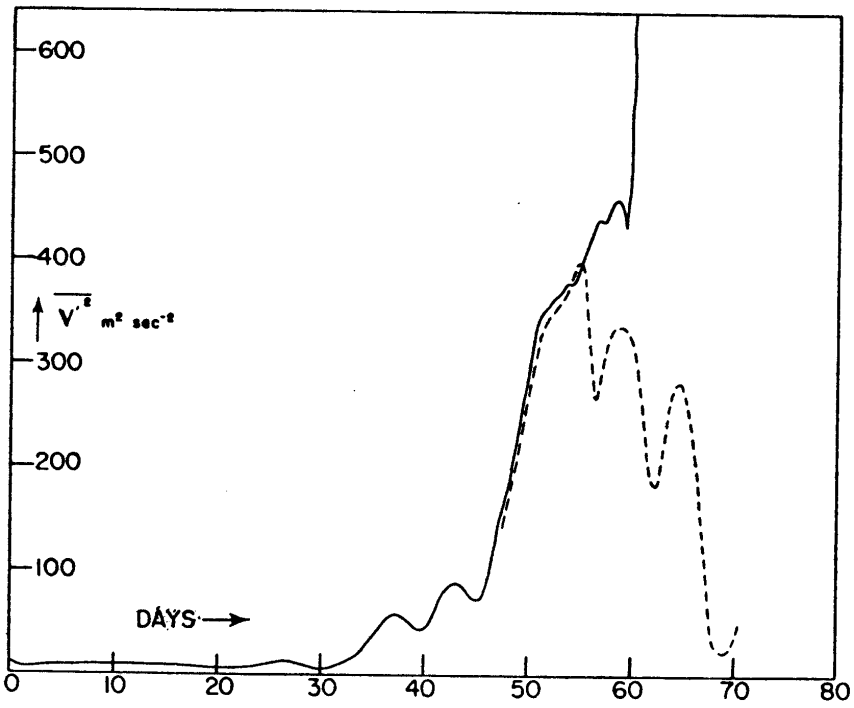

Fig. 1. Disturbance kinetic energy as a function of time. The solid curve was obtained without smoothing, the computations breaking down at about 56 days. The dashed curve was obtained by periodically introducing a filtering procedure.

Orszag (1971) later showed that it is sufficient to eliminate only waves equal to or shorter than $3\Delta x$ (see hand out).

The use of spectral filter is very expensive in grid point model. Doing it in spectral models is straightforward, however, since the solution is already in the spectral form.

4.3.3. Spatial Smoothing or Damping

In this case, we apply, at chosen intervals (often every time step), a spatial smoother similar in form to the term in our parabolic diffusion equation.

We want the smoothing to be selective, so that only the short (aliased) waves get damped.

Filter types:

Low-pass: allows low-frequency or long wavelength waves to pass through
High-pass: allows high-frequency or short wavelength waves to pass through
Band-pass: allows intermediate waves to pass through

What is desired here:

There exist many types of filters. Let look at one that is commonly used, the 1-2-1 or Shapiro filter:

$$\bar{u}_j = u_j + 0.5\upsilon(u_{j+1} - 2u_j + u_{j-1}) \qquad (2)$$

where the $\bar{u}_j$ is the value after smoothing.

To see what the smoother does, we need to look at the response function σ defined by

$$\bar{u} = \sigma u \, .$$

- all a filter does is changing the wave amplitude (a well-designed filter should not change the phase). Here σ might be a function of k, Δx, ν etc., much like $|\lambda|$ earlier.

The method for obtaining σ is very similar to the method for von Neumann stability analysis.

Let $u = A\exp(ikx_j)$. Plug it into (2) →

$$\bar{u} = [1 - \upsilon(1 - \cos(k\Delta x))]A\exp(ikx_j) \quad \rightarrow$$

$\sigma = [1 - \upsilon(1 - \cos(k\Delta x))]$ -- response function of filter (2).

See Figure.

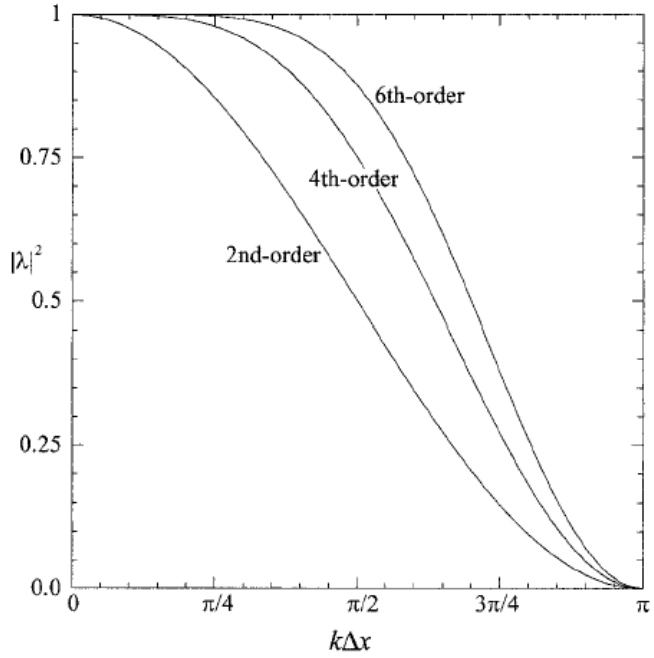

One can create multi-dimensional smoothers by successive applications of 1-D smoothers, one can also design fully MD ones.

4.3.4. Smoothing via numerical diffusion

This method damps the aliased waves by adding a smoothing or diffusion term to the prognostic equations (called computational mixing term in the ARPS – which also helps to suppress small scale noises created by dispersion and physical processes. Actually, ARPS uses advective formulations that conserve the advected quantities and their variances – therefore nonlinear instability due to aliasing is reasonably controlled even without the smoothing).

Consider for example of the CTCS case for linear advection:

$$\delta_{2t}u + \bar{u}\delta_{2x}u = \alpha \begin{bmatrix} -u \\ \delta_{xx}u \\ -\delta_{xxxx}u \\ \delta_{xxxxxx}u \end{bmatrix}^{n-1} , \qquad (3)$$

the right RHS terms are called zero, 2nd, 4th and 6th order numerical diffusion / smoothing, respectively. Note that the diffusion term is evaluated at time level n-1 – this makes the time integration forward in time relative to this term – remember that forward-in-time is (conditionally) stable for diffusion term but centered-in-time scheme is absolutely unstable.

We can find the response function to be

$$|\lambda|^2 = 1 - 2\alpha\Delta t \begin{cases} 1 \\ [2 - 2\cos(k\Delta x)]/\Delta x^2 \\ [6 - 8\cos(k\Delta x) + 2\cos(2k\Delta x)]/\Delta x^4 \\ [20 - 30\cos(k\Delta x) + 12\cos(2k\Delta x) - 2\cos(3k\Delta x)]/\Delta x^6 \end{cases} \qquad (4)$$

and they are plotted in the following figure. We can see that this term selectively damps shorter waves, and the higher order schemes are more selective, which is desirable. Given
$|\lambda|$, you can estimate the amplitude change due to the diffusion for different wavelength after given number of time steps.

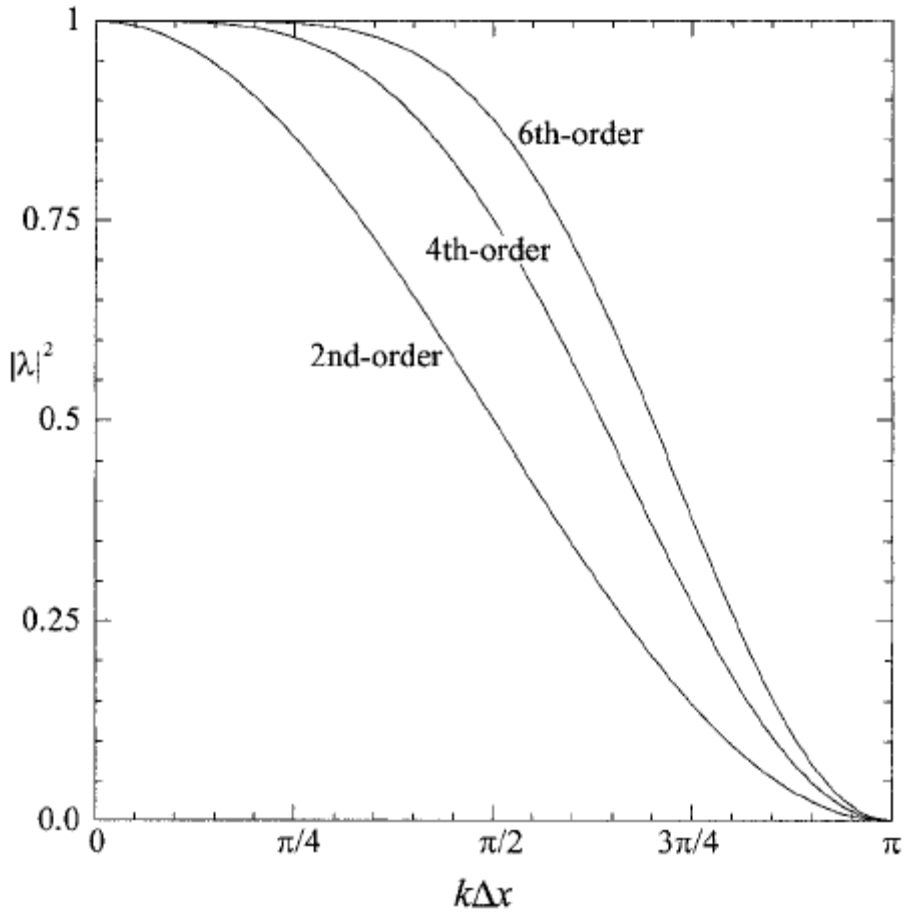

FIG. 1. Amplification factors $|\lambda|^2$ as given in Eq. (2) plotted against wavenumber ($k\Delta x$) for second-, fourth-, and sixth-order diffusion schemes. For each scheme, $\alpha\Delta t$ is chosen so that $|\lambda| = 0$ for $k\Delta x = \pi$, which corresponds to a wavelength of $2\Delta x$, i.e., the shortest waves representable on a discrete grid. In another word, $2\Delta x$ waves a completely damped after one time step of integration.

From Xue (2001, Mon. Wea. Rev.)

4.3.5. Lagrangian or Semi-Lagrangian Formulation

The cause of nonlinear instability is the nonlinear advection term in momentum equations. If we can get rid of this term, we can eliminate the instability!

This can be achieved by solving the advection problem in a Lagrangian or Semi-Lagrangian framework.

With Lagrangian methods, the pure advection problem is

$$\frac{du}{dt} = 0$$

i.e., u is conserved along the trajectory, which is also the characteristic curve ($dx/dt = c$) in this case.

In the purely Lagrangian method, the grid points move with the flow, and the grid can become severely deformed.

Semi-Lagrangian method is based on a regular grid – it finds the solution at grid points by finding the values of u at the departure points – the location where the parcels come from. Spatial interpolation is usually needed to find the value at the departure point. We will cover this topic in more details later.

4.3.6. Use of conservation to control nonlinear instability

Recall that aliasing acts to feed energy into small-scale components. It is possible to control (not prevent) aliasing by forcing the total energy or other physical properties (e.g., enstrophy – squared voroticity) to be conserved – just as the continuous system does.

If such constraints are satisfied, the energy spectrum cannot grow without bound!

Consider 2-D advection in a non-divergent flow:

$$\frac{\partial A}{\partial t} + u\frac{\partial A}{\partial x} + v\frac{\partial A}{\partial y} = 0 \qquad (5a)$$

$$\frac{\partial u}{\partial x} + \frac{\partial v}{\partial y} = 0 \qquad (5b)$$

We can write the advection-form equation (5a) in a flux-divergence form:

$$\frac{\partial A}{\partial t} + \frac{\partial (uA)}{\partial x} + \frac{\partial (vA)}{\partial y} = 0 \qquad (6)$$

What is conserved for this system of equations?

We first the domain integration of the first moment of A to be:

$$\frac{\partial}{\partial t}\left[\iint A dxdy\right] = -\iint \frac{\partial(uA)}{\partial x} dxdy - \iint \frac{\partial(vA)}{\partial y} dxdy$$
$$- \int [(uA)_L - (uA)_R] dy - \int [(vA)_T - (vA)_B] dx = 0 \qquad (7)$$

for a periodic domain. For non-periodic domain, we can see that the change in the domain integration of A equals to the net flux through the lateral boundaries – there is no interior source or sink in A.

We say the domain integral of the first moment of A is conserved by this system of equations.

Let's now look at the conservation of the second moment of A, i.e., A^2:

Multiply (6) by A→

$$A\frac{\partial A}{\partial t} + A\frac{\partial(uA)}{\partial x} + A\frac{\partial(vA)}{\partial y} = 0 \rightarrow$$
$$\frac{\partial}{\partial t}\left(\frac{A^2}{2}\right) + \frac{\partial(uAA)}{\partial x} + \frac{\partial(vAA)}{\partial y} - uA\frac{\partial A}{\partial x} - vA\frac{\partial A}{\partial y} = 0 \qquad (8)$$

Multiply (5a) by A →

$$\frac{\partial}{\partial t}\left(\frac{A^2}{2}\right) + uA\frac{\partial A}{\partial x} + vA\frac{\partial A}{\partial y} = 0 \qquad (9)$$

(8) + (9) →

$$\frac{\partial A^2}{\partial t} + \frac{\partial (uA^2)}{\partial x} + \frac{\partial (vA^2)}{\partial y} = 0 \qquad (10)$$

we have a conservation equation for A^2 in the flux divergence form too!

For a periodic domain, we have

$$\frac{\partial}{\partial t}\left[\iint A^2 dxdy\right] = 0$$

therefore the second-moment of A is also conserved by the continuous system.

What about the discrete equations? Do they also conserve these quantities? Not all discrete forms do. We will show one conservative example in the following.

Conservation for the Discrete System

Consider the case of staggered Arakawa C-grid:

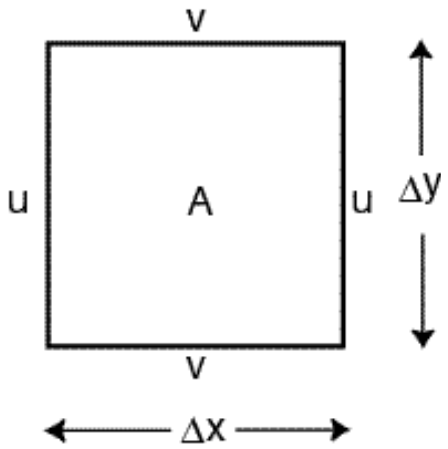

and the following second-order FD formulation:

$$\delta_{2t} A + \delta_x (u\overline{A}^x) + \delta_y (v\overline{A}^y) = 0 \qquad (11a)$$

$$\delta_x u + \delta_y v = 0 \qquad (11b)$$

Q: Does this system conserve A and A^2?

Note that $\overline{A}^x$ is defined at u point and $\overline{A}^y$ at v point, we denote $\overline{A}^x = B$ and $\overline{A}^y = C$ →

$$\sum_{ij} \delta_x (u\overline{A}^x) = (u_1 B_1 - u_0 B_0)/\Delta x + (u_2 B_2 - u_1 B_1)/\Delta x + ...$$
$$+ (u_{N-1}\ B_{N-1} - u_{N-2} B_{N-2})/\Delta x + (u_N\ B_N - u_{N-1} B_{N-1})/\Delta x = 0$$

with periodic B.C.

The same is true to the flux in y direction – therefore A is conserved.

Conservation of A^2 is a little more complicated to show. We will make use of two identities (you can check them out for yourself):

$$\delta_x(\bar{P}^x Q) = P\delta_x Q + \overline{(\delta_x P)Q}^x \qquad (12a)$$

$$\bar{P}^x \delta_x P = \delta_x(P^2/2) \qquad (12b)$$

Multiply (11a) by A→

$$A\delta_{2t}A = -A\delta_x(u\bar{A}^x) - A\delta_y(v\bar{A}^y) \qquad (13)$$

Look at only the 1st term on RHS of (13):

$$-A\delta_x(u\bar{A}^x)$$

Let $P = A,\ Q = u\bar{A}^x,$ (12a) becomes

$$\delta_x(\bar{A}^x u\bar{A}^x) = A\delta_x(u\bar{A}^x) + \overline{(\delta_x A)(u\bar{A}^x)}^x \rightarrow$$

$$A\delta_x(u\bar{A}^x) = \delta_x(\bar{A}^x u\bar{A}^x) - \overline{u\delta_x(A^2/2)}^x \qquad (14)$$

The 2nd term on RHS of (14) is not in the flux form. Using (12a) again, let $P = A^2/2$, $Q = u$

→ $$\delta_x(\overline{A^2/2}^x u) = (A^2/2)\delta_x u + \overline{\delta_x(A^2/2)u}^x$$

therefore

$$\overline{u\delta_x(A^2/2)}^x = \delta_x(\overline{A^2/2}^x u) - (A^2/2)\delta_x u \qquad (15)$$

Now (14) becomes

$$A\delta_x(u\bar{A}^x) = \delta_x(\bar{A}^x u\bar{A}^x) - \delta_x(\overline{A^2/2}^x u) + (A^2/2)\delta_x u \qquad (16)$$

- only the last term is not in the flux form.

For the *y* direction, we can also get

$$A\delta_y(v\bar{A}^y) = \delta_y(\bar{A}^y v\bar{A}^y) - \delta_y(\overline{A^2/2}^y v) + (A^2/2)\delta_y v \qquad (17)$$

(16) + (17) →

$$A\delta_x(u\bar{A}^x) + A\delta_y(v\bar{A}^y) = ... + (A^2/2)(\delta_x u + \delta_y v)$$

the last term is zero because of (11b)!

Therefore

$$\sum_{ij} A\delta_{2t}A = 0 \rightarrow \qquad \sum_{ij}(A^n A^{n+1} - A^{n-1}A^n) = 0 \rightarrow$$

$$\sum_{ij}(A^n A^{n+1}) = \sum_{ij}(A^{n-1}A^n)$$

$A^n A^{n+1}$ is not exactly A^2 due to the temporal discretization – we say A^2 is quasi-conserved!

Comments on Conservations:

- Conservation is generally a good thing to have in a model – can be used to check the correctness of code – if you know your scheme conserves, check if the domain integral changes in time.
- Don't want to use schemes that are known to conserve poorly.
- It is not always possible to conserve all conservative quantities of the continuous system, however.

Nonlinear advection schemes that conserve more quantities

Arakawa derived and compared several methods for dealing with the nonlinear advection of a barotropic vorticity equation

$$\frac{\partial \zeta}{\partial t} + u\frac{\partial \zeta}{\partial x} + v\frac{\partial \zeta}{\partial x} = 0 \qquad (18)$$

with $\zeta = \nabla^2\psi;\ u = -\frac{\partial \psi}{\partial y};\ v = \frac{\partial \psi}{\partial x}$

where ζ is vorticity and ψ is the streamfunction.

(18) can be rewritten as

$$\frac{\partial \zeta}{\partial t} - \frac{\partial \psi}{\partial y}\frac{\partial \zeta}{\partial x} + \frac{\partial \psi}{\partial x}\frac{\partial \zeta}{\partial y} = 0 \qquad (19)$$

where the advection can be written as a Jacobian:

$$J(\psi, \zeta) = \frac{\partial \psi}{\partial x}\frac{\partial \zeta}{\partial y} - \frac{\partial \psi}{\partial y}\frac{\partial \zeta}{\partial x} \qquad (20)$$

Arakawa came up with seven different forms of discretization for the Jacobian (called Arakawa Jacobians), some conserve total energy and enstrophy (ζ^2) (the PDE conserves both).

The following figures show total kinetic energy, total enstrophy and the kinetic energy spectrum, as function of time, using different Jacobians. Formulation No. 7 (J_7) is the only one that conserves both total energy and total enstrophy.

Three forms of the Jacobian and their finite difference counterparts

1'. $$J(\eta,\psi) = \eta_x\psi_y - \eta_y\psi_x \tag{5.46a}$$

$$J_1 = (\delta_{2x}\eta)(\delta_{2y}\psi) - (\delta_{2y}\eta)(\delta_{2x}\psi) \tag{5.46b}$$

$$J(\eta,\psi) = (\psi\eta_x)_y - (\psi\eta_y)_x \tag{5.47a}$$

$$J_2 = \delta_{2y}(\psi\delta_{2x}\eta) - \delta_{2x}(\psi\delta_{2y}\eta) \tag{5.47b}$$

$$J(\eta,\psi) = (\eta\psi_y)_x - (\eta\psi_x)_y \tag{5.48a}$$

$$J_3 = \delta_{2x}(\eta\delta_{2y}\psi) - \delta_{2y}(\eta\delta_{2x}\psi) \tag{5.48b}$$

It was shown by Arakawa (1966) that the Jacobian J given by

$$J = \alpha J_1 + \gamma J_2 + \beta J_3 , \quad \alpha + \gamma + \beta = 1 , \qquad (59)$$

conserves mean square vorticity if $\alpha = \beta$ and conserves energy if $\alpha = \gamma$. Examples of Jacobians which have the form of (59) are

$$J_4 = \frac{1}{2}(J_1 + J_2) ,$$

$$J_5 = \frac{1}{2}(J_2 + J_3) ,$$

$$J_6 = \frac{1}{2}(J_3 + J_1) ,$$

$$J_7 = \frac{1}{3}(J_1 + J_2 + J_3) . \qquad (60)$$

A schematic representation of the ζ and ψ points used in constructing the seven finite-difference Jacobians introduced above is given in Fig. 11.

J_7 is the Jacobian proposed by Arakawa (1966) as conserving both enstrophy and energy. J_2 and J_6 conserve enstrophy, but not energy. J_3 and J_4 conserve energy,

but not enstrophy. All five schemes mentioned thus far are stable. J_1 does not conserve either quantity. J_5, also, does not conserve either quantity, but experience with numerical tests shows that the instability is very weak, if it exists at all. This is not surprising, since $2J_5 = 3J_7 - J_1$; because J_7 is a quadratic-conserving scheme the time rates of change of the mean quadratic quantities using J_5, for given ζ and ψ, have opposite sign to the time rates of change of the mean quadratic quantities using J_1.

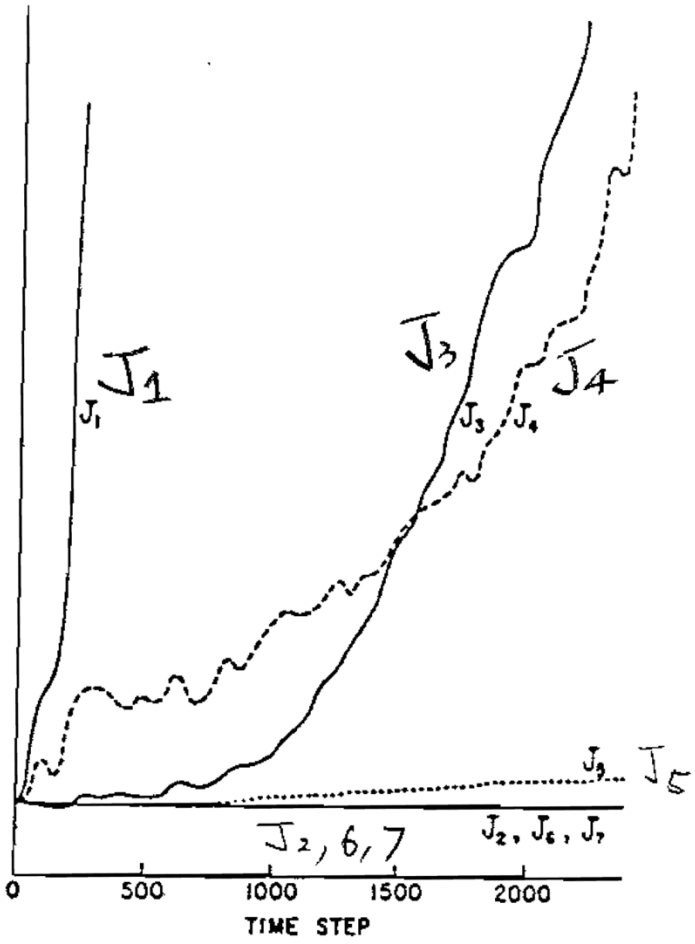

(conserves enstrophy or vorticity sqaured)

FIG. 12. Comparison of the time variation of the mean square vorticity (units arbitrary) during a numerical integration with the seven finite-difference Jacobians under consideration. (Arakawa, 1970). Reprinted with permission of the publisher American Mathematical Society from *SIAM-AMS Proceedings*. Copyright © 1970, Vol. 2, Fig. 5, p. 35.

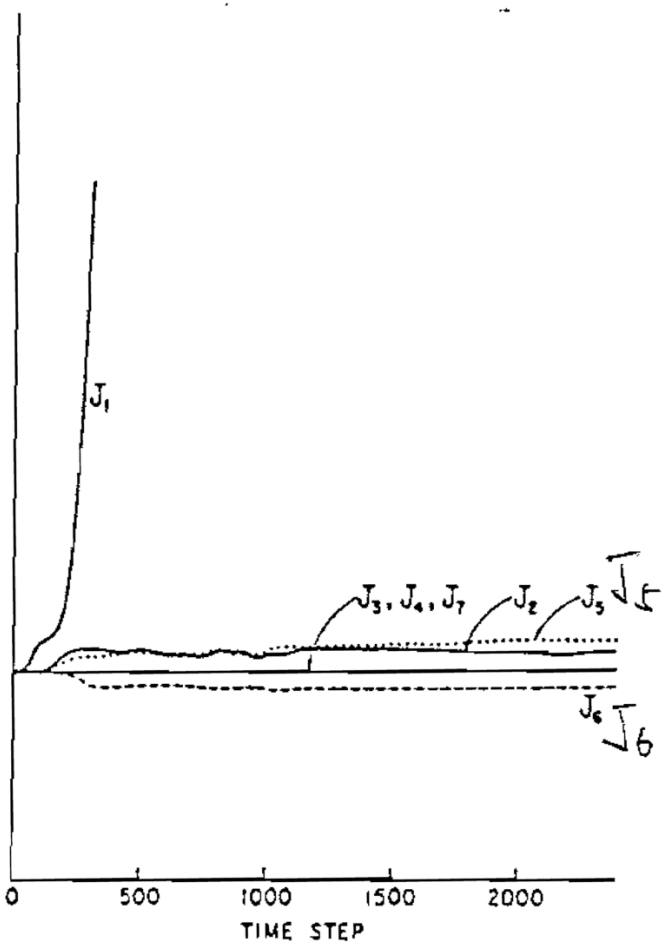

Conserves kinetic energy

FIG. 13. Comparison of the time variation of the kinetic energy during a numerical integration with the seven finite-difference Jacobians under consideration (Arakawa, 1970). Reprinted with permission of the publisher American Mathematical Society from *SIAM-AMS Proceedings*. Copyright © 1970, Vol. 2, Fig. 6, p. 36.

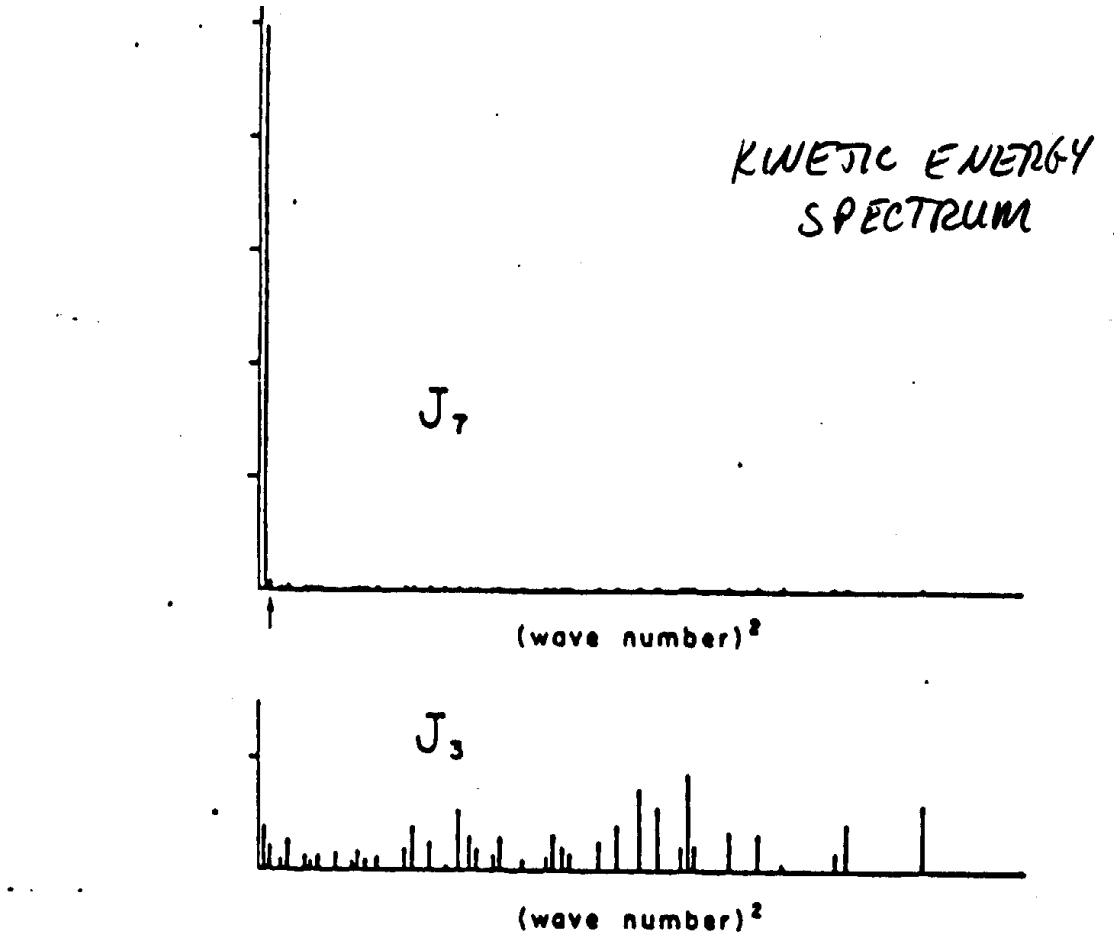

FIG. 14. A comparison of the spectral distribution of kinetic energy, obtained with J_3 and J_7, after a numerical integration of 2400 time steps. Arrow shows the wave number that contained most of the energy at the initial time.

Read Mesinger and Arakawa (1976) GARP Report, section 7 of Chapter 3.

Figure 14 shows the spectral distribution of kinetic energy obtained by the energy and enstrophy conserving scheme J_7 and by the energy conserving scheme J_3 at the end of the calculations. The small arrow shows the wave number for $\sin(\pi i/8)\cos(\pi j/8)$, which contained almost all of the energy at the initial time. Although the total energy was approximately conserved with J_3 there was a considerable spurious energy cascade into the high wave numbers, whereas with J_7 more energy went into a lower wave number than into the higher wave numbers, in agreement with the conservation of the average wave number as given by Eq. (52).

Whether the increase of the enstrophy is important in the simulation of large-scale atmospheric motion will depend on the viscosity used with the complete equation. A relatively small amount of viscosity may be sufficient to keep the enstrophy quasi-constant in time. However, the viscosity will also remove energy, and as a result the average wave number, defined by Eq. (52), will falsely increase with time.